ADVANCES IN MATERIALS SCIENCE, Vol. 25, No. 4 (86), December 2025

DOI: 10.2478/adms-2025-0020

Yacine Halouane[1], Omprakash Varma Etrouth[1], Gazel Abilezova[2*], Fuad Khoshnaw[1*]

[1]*School of Engineering, Infrastructure and Sustainability, De Montfort University, Leicester, LE1 9BH, United Kingdom*
[2]*Mechanical Engineering Department, Satbayev University, Almaty, Kazakhstan*

* *fuad.khoshnaw@dmu.ac.uk*

EXPERIMENTAL INVESTIGATION OF PROCESS PARAMETERS ON SURFACE AND MECHANICAL PERFORMANCE OF 3D PRINTED PARTS

ABSTRACT

This study examines the influence of print orientation and printing speed on the mechanical strength and surface roughness of components fabricated from Polylactic Acid (PLA) using the Fused Deposition Modeling (FDM) process. The 3D-printed samples were produced with varying orientations (0°, 90°, and 45°) and print speeds, while other parameters remained constant. All samples had a 100% infill density, a "Lines" infill pattern, and a printing temperature of 210°C. The 0° and 90° samples were printed at 50 mm/s, whereas the 45° samples were printed at 40, 60 and 80 mm/s. Each sample was printed three times to ensure repeatability and obtain an average result. The results indicate that raster angle plays a critical role in determining mechanical performance, with 0° and 90° orientations yielding the highest 72.31 MPa and lowest 56.26 MPa stress values, respectively. Additionally, a nuanced relationship was observed between printing speed, surface roughness, and tensile strength. Surface roughness metrics, including Ra, Rz, and Rq, improved with decreasing printing speed, indicating enhanced surface finishes. The optimal tensile strength of 57.95 MPa was achieved at a moderate printing speed of 60 mm/s, offering the best balance between mechanical strength and surface quality. This research enhances the understanding of parameter optimisation in FDM processes, providing practical insights for the production of high-performance PLA-based components.

Keywords: *additive manufacturing, PLA, printing parameters, printing orientation, surface roughness*

INTRODUCTION

Additive manufacturing, or 3D printing, is a transformative technology that creates three-dimensional objects by layering material based on digital designs. Unlike traditional methods that remove material, 3D printing adds material, enabling the production of complex geometries and intricate details [1-3]. This technology has revolutionized industries like aerospace, healthcare, and consumer goods by enabling faster prototyping, customization, and on-demand production. As it becomes more affordable, 3D printing is increasingly accessible, empowering businesses and individuals to innovate and redefine manufacturing [4-6]. Over the years, researchers [7-10] have studied the strength and fracture behavior of additively manufactured parts due to their exposure to diverse stress conditions in real-world

Received: 31.05.2025; Received in revised form: 01.08.2025; Accepted: 06.11.2025

applications. With the rapid growth of 3D printing in recent years, numerous engineering components have been extensively studied in this field [11-14].

Other researchers investigated the influence of technological parameters on 3D printing and the optimization of manufacturing parameters for PLA components using Taguchi and Neural Network techniques. Their findings demonstrated the potential to optimize the mechanical characteristics of printed parts through appropriate adjustment of 3D printing parameters while minimizing production costs. The study specifically examined the effect of various printing process parameters on the impact strength of parts fabricated with PLA filament [15-16]. Issametova et al. [17] determined residual stresses in 3D-printed polymer parts and composites using a combination of bridge curvature, optical scanning, and finite element methods. Li et al. [18] conducted experimental and computational research on 3D-printed polymers. Using the fused deposition modeling (FDM) technique, they fabricated single-edge notch tension samples from acrylonitrile-butadiene styrene (ABS). Tests on samples with varying raster orientations revealed that raster orientation significantly affected fracture properties. The study also suggested that surface topological patterns could enhance the strength and fracture toughness of components. Studies have shown that optimizing printing parameters, such as raster angle, orientation, and print speed, can significantly enhance the tensile properties of 3D-printed components. For example, a smaller layer height improves layer adhesion, boosting tensile strength. Adjusting the raster angle helps distribute applied loads more uniformly, reducing stress concentrations and enhancing overall strength. Additive manufacturing, particularly 3D printing, has revolutionized production by enabling near-net-shape geometries with minimal waste. Among the factors affecting the quality of 3D-printed parts, print speed is particularly critical [19].

The tensile strength of 3D-printed parts is heavily influenced by print layer orientation, a critical factor for ensuring structural integrity and durability in applications. Printing orientation, defined by the alignment of layers relative to the build platform, significantly affects mechanical properties. Parts with layers printed perpendicular to the applied force generally exhibit higher tensile strength compared to those printed parallel to the force. This variation arises from differences in interlayer bonding strength and the anisotropic nature of materials inherent to the 3D printing process [20]. The capabilities of 3D printing technology are rapidly expanding. Fused Deposition Modeling (FDM), also known as Fused Filament Fabrication (FFF), has become a leading method in solid-based additive manufacturing due to its low cost, ease of use, and compatibility with a growing range of materials, such as polylactic acid (PLA), polypropylene (PP), polyethylene terephthalate glycol (PETG), and acrylonitrile butadiene styrene (ABS) [21]. Its cost-effectiveness and user-friendly operation make FDM particularly appealing for beginners, driving its widespread use in educational institutions, public libraries, and office settings.

The FDM process begins with designing a digital 3D model using Computer-Aided Design (CAD) software. This model is then processed through slicing software, dividing it into layers and configuring printer parameters before transmitting the data to the printer. The FDM method works by extruding molten thermoplastic through a heated nozzle, building the object layer by layer. Thermoplastics in filament form are the primary materials used, transitioning from solid to liquid during printing. While most FDM printers currently support single-material, single-color printing, advancements in multi-material technology are expected to enhance FDM's capabilities and applications [22].

The study of tensile properties in 3D-printed materials has gained prominence due to the growing adoption of additive manufacturing across industries. Research highlights key factors affecting tensile strength, including printing parameters, material types, print orientation, printing speed, and post-processing techniques. Increasing the nozzle speed from 30 mm/s to

60 mm/s reduces the cooling period between applied fibers or layers, negatively affecting the polymer's crystallinity. This results in lower crystallization and a decrease in tensile strength [23]. Additionally, the raster pattern directly influences strength, weight, printing duration, and accumulated stresses, which can lead to crack formation and delamination [24–25].

The mechanical properties of 3D-printed parts are heavily influenced by printing parameters. Casavola et al. [26] showed that smaller layer heights improve tensile strength by enhancing layer adhesion and minimizing voids. Similarly, Mohamed et al. [27] observed that higher printing speeds reduce tensile strength due to insufficient bonding time between layers, weakening interlayer adhesion. These studies highlight the need to optimize printing parameters for desired mechanical properties. Print orientation also plays a significant role in tensile performance. Tymrak et al. [28] found that parts printed along the Z-axis exhibit lower tensile strength than those printed along the X-axis, due to weaker interlayer bonding in the vertical direction. The anisotropic nature of 3D-printed parts underscores the importance of considering print orientation during design and manufacturing to achieve optimal mechanical performance.

Material selection significantly impacts the tensile properties of 3D-printed parts. Wong and Hernandez [29] found that ABS generally exhibits higher tensile strength than PLA due to superior interlayer bonding, making it suitable for high-performance applications. Composite materials further enhance tensile properties, as demonstrated by Tekinalp et al. [30], who showed that adding carbon fibres to PLA matrices improves tensile strength and modulus, highlighting the potential of material innovation for high-strength applications. PLA is widely used for its smooth finishes and ease of printing, making it ideal for rapid prototyping and low-stress applications such as decorative items and storage containers [31]. Its resistance to warping, due to a low thermal expansion coefficient, is another advantage [32]. Additionally, Koslow [33] notes that PLA is safer than ABS, as it does not release harmful fumes during printing. However, PLA has limitations. Its low melting point and heat sensitivity make it unsuitable for high-temperature applications, as items can deform in environments like dishwashers [32, 34]. PLA is also more brittle and less flexible compared to materials like ABS or Nylon. Furthermore, its safety for food-related applications can be compromised when additives are used, and its tendency to absorb moisture requires careful storage [33].

Wang et al. [35] analysed FDM process parameters and their effects on PLA’s mechanical properties, revealing that factors like printing angle, layer thickness, fill rate, and nozzle temperature significantly influence tensile strength. Their findings underscore the importance of optimizing these parameters to achieve desired mechanical characteristics in FDM-printed PLA components. However, other researchers [36] formulated that printing speed and orientation do not have a statistically significant effect on the mechanical strength, durability, surface roughness, or overall quality of 3D-printed PLA parts. This hypothesis was tested by employing fused deposition modelling (FDM) to evaluate the influence of different printing speeds and orientations on the tensile strength and surface roughness of PLA samples. The experimental results demonstrated that mechanical strength decreased at higher printing speeds, particularly above 80 mm/s, and that samples printed along the X-axis exhibited higher impact and tensile strength compared to those printed along the Y- and Z-axes. Furthermore, tensile strength decreased by approximately 36% at a vertical angle (90°) compared to flat orientations (0°), indicating that lower printing angles generally enhanced strength due to alignment with the print direction.

Despite extensive research on the mechanical behaviour of 3D-printed PLA, the effects of specific printing angles on the X, Y, and Z axes remain underexplored. This study addresses this gap by analysing the tensile properties of neat PLA samples printed at varying inclination angles using the FDM process, with a focus on comparing their mechanical performance. Additionally, this paper investigates the impact of print speed on the surface finish and tensile strength of 3D-printed parts. Understanding this relationship is crucial for achieving desired quality and performance in applications such as prototyping, manufacturing, biomaterials, aerospace and automotive industries.

MATERIALS AND EXPERIMENTAL WORKS

PLA material was used in this study with the Prusa MK4 3D printer. Tensile tests were conducted using the Instron 6800 Series Testometric machine, and the resulting data were analysed to generate stress-strain curves, facilitating the calculation of key mechanical properties. The samples were printed using the Prusa MK4 3D printer, which employs Fused Deposition Modelling (FDM) technology - the most widely adopted method in additive manufacturing. The printer's user-friendly design and reliability make it ideal for producing consistent, high-quality prints. PrusaSlicer software was used to convert the CAD file of the samples into STL format, ensuring compatibility with the 3D printer. This critical step enabled accurate interpretation of the digital models.

During the slicing process, the CAD file was converted into G-code, a set of detailed instructions for the 3D printer, including the movements of the nozzle and bed. Following these instructions, the printer deposited material layer by layer to construct the physical object based on the digital design. By adhering to this structured process, the study ensured precise and reliable sample preparation for tensile testing.

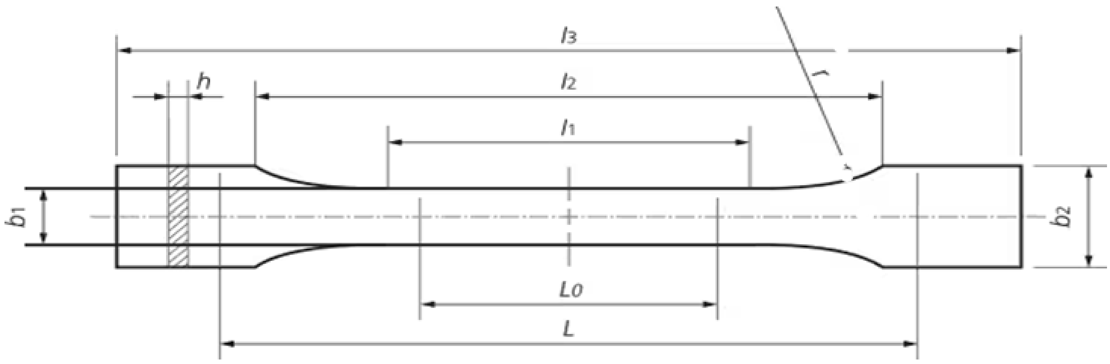

Fig. 1. Sample type and dimensions

The tensile test samples were designed according to the ASTM D638 (TYPE I) standard, a widely recognised guideline for evaluating the tensile properties of plastics. This standard ensures consistency and comparability of results by specifying the shape and dimensions of the samples. Figure 1 and Table 1 show the dimensions of the sample. This standard was selected for the study due to its suitability for 3D-printed plastics, ensuring an accurate representation of the material's mechanical properties.

Table 1. *Sample design dimensions*

Properties	Values (mm)
L_0	50.0
l_1	57.0
l_2	115.0
l_3	165.0
H	3.2
R	76
b_1	13
b_2	19

The 3D-printed samples were fabricated using FDM with variations in printing orientation and speed while maintaining constant printing parameters. All samples were printed with an infill density of 100%, a "Lines" infill pattern, and a printing temperature of 210°C. The samples were printed at three orientations: 0°, 90°, and 45°. The printing speed was set at 50 mm/s for the 0° and 90° orientations, while for the 45° orientation, additional samples were printed at varying speeds of 40, 60, and 80 mm/s. Each sample was printed three times using the same parameters to ensure repeatability and to obtain an average result. The detailed process parameters are presented in Table 2.

Table 2. *3D Printing parameters for sample fabrication*

Printing Orientation (^{0}) Degree	Print Speed (mm/sec)
0	50
90	50
45	40
45	60
45	80

Mechanical Properties

The tensile test for the printed samples was carried out using a Testometric machine (Instron 6800 Series). Throughout the testing process, the sample was firmly clamped between the grips of the machine, and essential parameters were set for the test. The primary goal of this tensile test was to assess the material's strength, stiffness, and elongation until it reached its breaking point. The Testometric software also automatically generated a stress-strain curve based on the initial gauge length (L_0) and the cross-sectional area ($A = b_1 \times h$), which were specified before the test began. The testing was conducted at a speed of 50 mm/min, with the machine recording critical data such as the applied force and the displacement of the sample throughout the experiment. Stress and strain were calculated to analyze the mechanical properties of the material using recorded displacement and force data, which included columns for time, displacement, and force. The data was imported into Excel for preprocessing, where relevant columns were prepared for analysis. Strain (ε), representing the elongation per unit length of the material, was then calculated using the formula 1:

$$\epsilon = \frac{\Delta L}{L} \times 100 \tag{1}$$

where:
ΔL is the displacement in millimetres (mm);
L is the original length of the sample, which was 50 mm.

To facilitate easier interpretation, the strain was converted into a percentage by dividing the change in length (ΔL) by the original length (L_0) and multiplying by 100.
Stress (σ), which measures the internal forces within the material per unit area, was then calculated using formula 2:

$$\sigma = \frac{F}{A} \tag{2}$$

where:
F is the force applied to the material in N
A is the original cross-sectional area of the sample, which equals 41.6 mm^2
The resulting stress values were expressed in N/mm^2 (MPa).

The modulus of elasticity, also called Young's modulus, was determined from the initial linear portion of the stress-strain curve, representing the material's elastic behavior where stress and strain have a linear relationship. The linear region, typically within the first 0.5% to 1% strain, was identified as it reflects elastic behavior before plastic deformation. The slope of this region was then calculated to determine the modulus of elasticity, using the following formula 3:

$$E = \frac{\Delta\sigma}{\Delta\epsilon} \tag{3}$$

where:
E is the modulus of elasticity, in Pa;
$\Delta\sigma$ is the change in stress within the linear region, in Pa;
$\Delta\epsilon$ is the change in strain within the linear region, unitless.

The modulus of elasticity was determined by dividing the change in stress by the corresponding change in strain within the identified linear region.

Toughness Calculation

Toughness, representing the energy a material absorbs until fracture, was determined from the area under the stress-strain curve. The curve, plotted with strain on the x-axis and stress on the y-axis, was analyzed using software tools to estimate the total area up to the fracture point. This analysis provided insights into the material's energy absorption capacity before failure. The toughness was extracted from the plotted stress-strain diagram by first generating the curve as described in the previous section, with strain represented on the x-axis and stress on the y-axis. The area under the stress-strain curve, which corresponds to the toughness, was then visually identified and estimated using appropriate software tools. This area represents the total energy absorbed by the material during deformation up to the point of fracture.

Surface Roughness

The data analysis method applied in this research involves a methodical approach of examining the results on surface roughness and tensile strength to determine the effect of modified print speed on 3D-printed PLA. The data collected for the surface roughness and tensile strength tests are then made systematic. By print speed, the results of surface roughness parameters such as average roughness (Ra), peak to valley height (Rz), root mean square roughness (Rq) and tensile strength of the produced samples are categorized. This makes it easier to compare results that have been obtained at different print speeds. Finally, the implications of the statistical analysis results are provided to conclude the appropriate print speed setting. Such conclusions will aid in making recommendations on how to achieve the optimal surface finish and mechanical properties in 3D printing, particularly when using PLA material.

Taylor-Hobson Form Talysurf Intra Touch was used in surface roughness measurement and the mechanical properties of the printed samples were tested using the tensile testing machine. The above tools yielded high-accuracy data, which was very crucial in the subsequent analysis and vindication of the results of the experiment. To the extent that the study was successful, it was achieved through a cautious process of putting into practice and enhancing the mentioned and above processes to yield preferable, reliable and replicable outcomes.

RESULTS

Effect of Orientation

The initial phase of the results section introduces the 3D-printed samples prepared for the tensile stress tests. Figures 2a and 2b illustrate the samples printed at two distinct orientations, 0° and 90°, respectively. These orientations were selected to assess how the printing direction influences tensile strength. The 0° orientation samples were printed with their layers aligned parallel to the loading direction, while the 90° orientation samples were printed with their layers perpendicular to the loading direction. Figure 3 shows samples of 0° orientation after tensile testing.

a) 0° orientation

90° orientation

Fig. 2. 3D printed samples

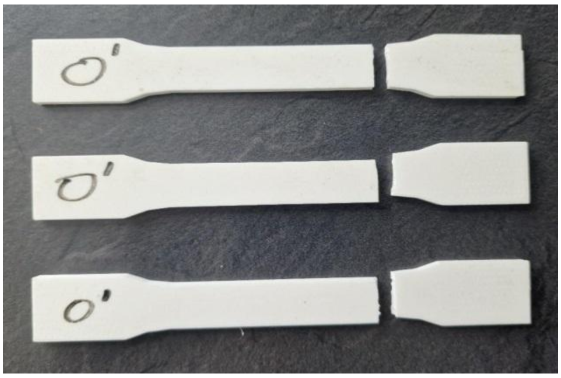

Fig. 3. Samples of 0° orientation after tensile testing

Figures 4a and 4b illustrate Force - Displacement and Stress-Strain curves, respectively. For each experiment, three samples were tested, and the average was taken. Maximum force is 3032 N and displacement is 3.33 mm. The average stress, Young's modulus, strain, and toughness were 72.31 MPa, 2013.33 MPa, 6.33%, and 6.53 N·m, respectively.

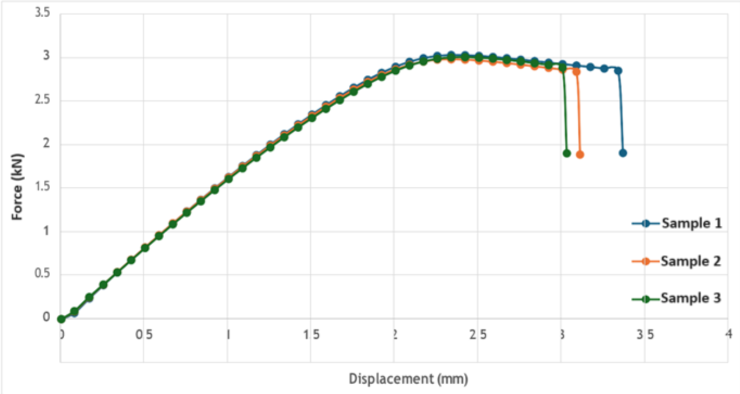

a: Force vs. Displacement diagrams

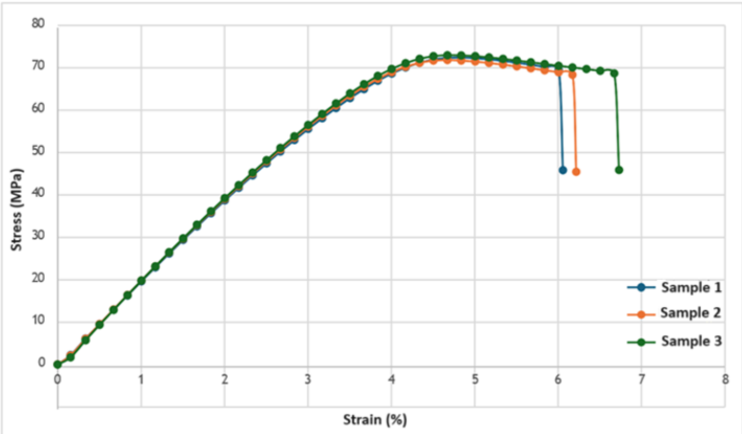

b: Stress vs. Strain diagrams

Fig. 4. Force – Displacement and Stress – Strain diagrams for samples of 0° orientation

Figure 5 shows the fracture details for the samples of 90° orientation samples after tensile testing.

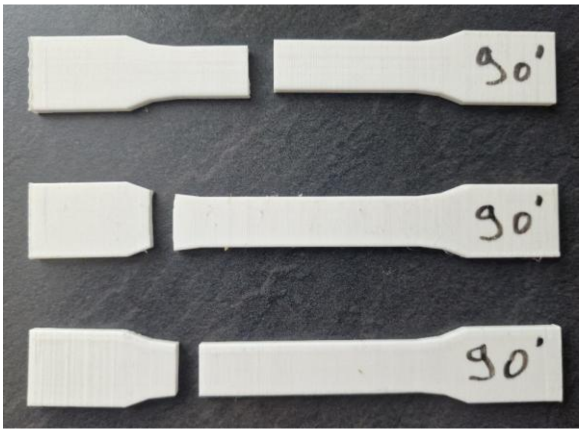

Fig. 5. Samples of 90° orientation after tensile testing

Figures 6a and 6b show Force - Displacement and Stress - Strain curves, respectively. Maximum force is 2422 N and displacement is 1.835 mm. The average stress, modulus of elasticity, strain, and toughness were 56.26 MPa, 1834 MPa, 3.49%, and 2.21 N·m, respectively.

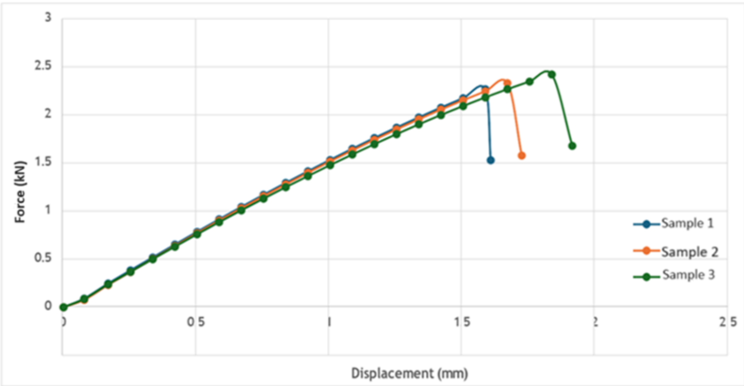

a: Force vs Displacement diagrams.

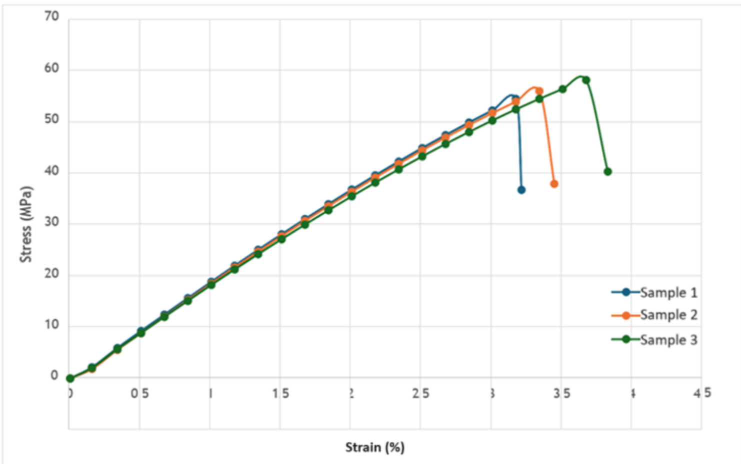

b: Stress vs Strain diagrams.

Fig. 6. Force – Displacement and Stress – Strain diagrams for Samples of 90° orientation

Table 3 shows Young's modulus and toughness results after testing samples with 0° and 90° orientation

Table 3. *Mechanical properties of samples with 0° and 90° orientation*

Printing at 0° Orientation			Printing at 90° Orientation		
Sample No	Young modulus (GPa)	Toughness (N.m)	Sample No	Young modulus (GPa)	Toughness (N.m)
1	1.98	6.11	1	1.86	1.92
2	2.01	6.35	2	1.83	2.16
3	2.03	7.15	3	1.79	2.56
Average	2.01	6.53	Average	1.83	2.21

Effect of Speed

The next group of samples was also produced using FDM printer technology, which involved simultaneous printing of objects to ensure that the sample was obtained. All the test samples were printed using PLA filament, and the only difference between these samples was the printing speed. Other variables that could cause interference, such as ambient temperature and humidity, were also kept constant for proper control to achieve the expected print quality and mechanical performance. After the print is complete, the samples are allowed to stabilize, and then measurements of surface roughness are taken. The surface roughness of each specimen was measured using a Taylor Hobson Form Talysurf Intra Touch profilometer (Figure 7a). Before each test, the instrument was calibrated to minimize measurement errors. During measurement, each specimen was placed on the testing platform with the stylus in contact with the surface. Measurements were taken multiple times across different regions of each specimen, with the stylus traversing to the printed layer lines (Figure 7b), to capture the surface roughness directionally. The recorded data included Ra (average roughness), Rz (mean roughness depth), and Rq (root mean square roughness), providing a comprehensive assessment of the surface finish.

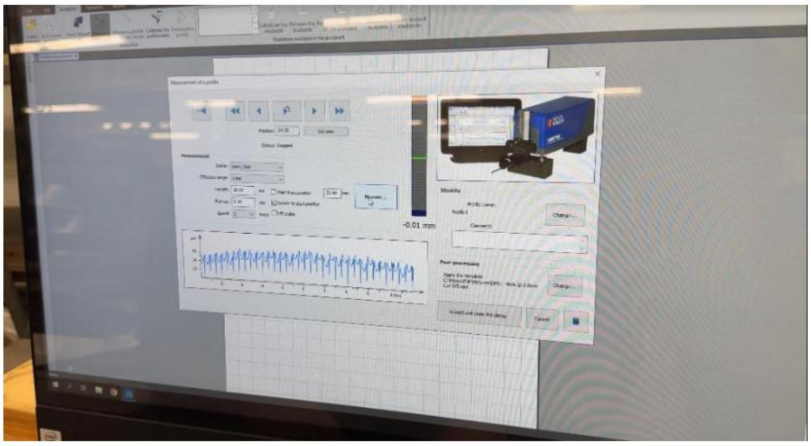

a: Surface roughness simulation Talysurf Intra Touch

b: Surface roughness setup

Fig. 7. Surface roughness measurement and simulation setup

Table 4 shows the average roughness test results of the samples. The results and analyses of the surface roughness test section describe in detail how the variation in print speeds influences the surface finish of the samples made from 3D-printed PLA. Surface roughness for each three samples was measured using a Taylor Hobson Form Talysurf Intra Touch profilometer, and all measurements had some roughness key parameters recorded, such as average roughness (Figure 7b).

Table 4. *Roughness test results*

	Average amplitude parameters for samples									Material ratio parameters	
№	R_p (μm)	R_v (μm)	R_z (μm)	R_c (μm)	R_t (μm)	R_a (μm)	R_q (μm)	R_{sk}	R_{ku}	R_{mr} %	R_{dc} (μm)
40 mm/s	9.40	6.99	16.41	10.54	23.15	2.61	3.28	0.72	3.44	0.22	5.19
60 mm/s	11.33	5.93	17.26	11.14	25.36	2.75	3.59	1.09	4.14	0.15	5.16
80 mm/s	7.69	18.41	26.10	16.47	36.82	2.91	4.47	-1.56	7.37	0.30	4.36

The key parameters measured include:

- Ra (Average Roughness): The average value of the heights of the surface and this is therefore used to give a general outlook of the surface texture.
- Rz (Mean Roughness Depth): The ratio of the Arithmetic mean of the five tallest peaks within the measurement span and the five deepest troughs as a summary of the surface's peak-to-valley profile.
- Rq (Root Mean Square Roughness): A more sensitive value highlighting the fluctuation in the surface is obtained by the mean square root of the deviation.

Mechanical Properties

This part will describe the influence of applying different print speeds on the mechanical strength of the 3D-printed PLA samples. Tensile strength testing was conducted using a tensile test machine; maximum load, break load, and extension at break were among the most important parameters measured. Table 5 illustrates the average values of samples after tensile testing.

Table 5. *Average tensile test results of samples*

Sample Printing Parameters	Ultimate Tensile Stress MPa	Fracture Stress MPa	Max. Strain (ε)
40 mm/s	53.96	49.85	8.08
60 mm/s	57.95	52.26	9.83
80 mm/s	55.61	45.43	9.17

Every sample is printed in a separate batch to avoid different results because of variations in print settings. The print speed is set for every batch of samples, starting from slow to fast print speeds, such as low = 40 mm/s, while high = 80 mm/s.

Figures 8a and 8b illustrate samples after the tensile strength test of the top and side views. Lastly, the study incorporates only standardized geometries that are relatively simple for the test samples.

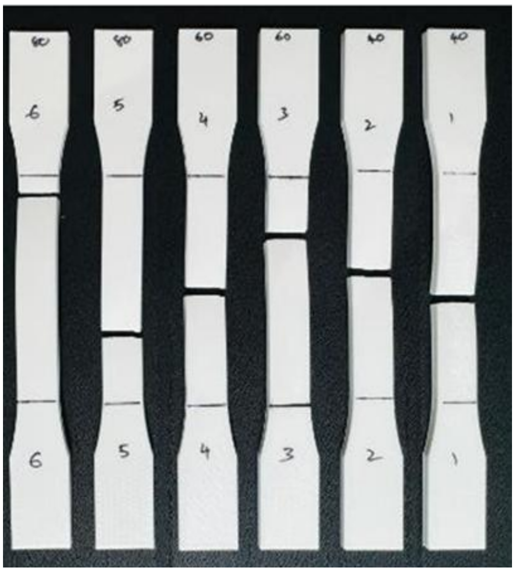

a: After the tensile strength test of 8 models (Top view)

b: After the tensile strength test of 8 models (Side view)

Fig. 8. Post-tensile test views of samples

DISCUSSION

The results of the first group of samples (Figures 6a and 6b) in this study provide detailed insights into the effect of printing orientation on the tensile strength, toughness, and Young's modulus (Table 3) of 3D printed parts using FDM. The tensile tests revealed that samples printed at 0° orientation, where the layers are aligned parallel to the applied load, exhibited significantly higher tensile strength, with an average stress of 72.31 MPa. In contrast, samples printed at 90°, where the layers are perpendicular to the load, demonstrated an average stress of 56.26 MPa. This substantial difference underscores the anisotropic nature of FDM-printed materials, where the mechanical properties are highly dependent on the direction of the applied force relative to the orientation of the print layers. The higher tensile strength observed in the 0° orientation can be attributed to the alignment of the extruded material with the direction of the applied load. In this configuration, the continuous strands of filament are capable of directly resisting the tensile force, resulting in a more efficient transfer of stress along the length of the sample. This direct alignment allows for better distribution of the load across the entire material, minimizing weak points and enhancing the overall tensile strength. The average stress of 72.31 MPa in the 0° samples reflects this optimal load-bearing capacity. In contrast, the 90° orientation exhibits weaker tensile strength due to the reliance on interlayer adhesion, which is inherently less robust than the intralayer bonding within each layer of material. In this orientation, the applied force acts perpendicular to the layers, placing stress on the interfaces between them. These interlayer bonds are formed as successive layers of material cool and solidify, but the bonding process is not as strong as the material's internal cohesion. The average stress of 56.26 MPa in the 90° orientation highlights (Figure 6b) the challenges associated with this configuration, where the mechanical integrity is more prone to failure under tensile loading due to weaker layer bonding.

Toughness, which measures the energy a material can absorb before fracturing, further illustrates the differences between the two orientations. The 0° samples exhibited a higher average toughness of 6.53 N.m, compared to 2.21 N.m for the 90° samples (Table 3). This significant disparity in toughness indicates that the 0° orientation is not only stronger but also more ductile and capable of absorbing more energy before failure. The higher toughness of the 0° samples can be attributed to the continuous filament alignment, which allows the material to deform more uniformly under stress. In contrast, the lower toughness in the 90° orientation is due to the weaker interlayer bonds, which are more prone to brittle failure when subjected to tensile forces.

Young's modulus, a measure of material stiffness, also showed variation between the two orientations. The 0° samples had an average Young's modulus of 2.01 GPa, while the 90° samples had a lower average modulus of 1.83 GPa (Table 3). This difference in stiffness further emphasizes the anisotropic nature of FDM-printed parts. The higher modulus in the 0° orientation suggests that the material resists deformation more effectively when the load is applied along the continuous strands of filament. Conversely, the lower modulus in the 90° orientation indicates that the material is more prone to deformation when the load is applied across the weaker interlayer bonds.

These findings align with previous studies in the field and support the hypothesis, confirming that print orientation is a critical factor influencing the mechanical properties of FDM-printed parts. Tymrak et al. [28] and Wang et al. [35] both reported similar trends, where samples printed with layers parallel to the loading direction exhibited higher tensile strengths, greater toughness, and higher stiffness compared to those printed perpendicular to the load. The alignment between the results of this study and those reported in the literature further strengthens the understanding that anisotropy is a fundamental characteristic of FDM-printed materials. The consistency of these findings across different studies suggests that the anisotropic behavior observed is not an isolated phenomenon but a general property of parts produced using FDM technology.

While the results are like previous experiments [28,35], they also highlight important aspects that must be considered when optimizing print settings. The quality of layer adhesion is particularly crucial in influencing tensile strength, toughness, and stiffness, especially in orientations like 90°, where the load is applied across layers. Factors such as nozzle temperature, print speed, and cooling rate all contribute to the effectiveness of layer bonding. If these parameters are not properly optimized, they can lead to insufficient adhesion between layers, which in turn reduces the mechanical properties. For example, a nozzle temperature that is too low might not provide enough heat to ensure proper fusion between layers, while a temperature that is too high could degrade the material, weakening the overall structure.

The second group of samples' roughness test results (Table 3 and Figures 7a,7b) showed the relationship between print speed and surface roughness, as the slower the print speed, the smoother the sample's surface. This was reflected by a lower magnitude of Ra, Rz, and Rq values relative to print speed.

In this study, the relationship between print speed and mechanical strength was found to be non-linear. Samples printed in the mid-speed range of approximately 50–70 mm/s achieved the highest tensile strength, with maximum stress values reaching 58.32 MPa. Samples printed at 60 mm/s demonstrated the most favourable balance, exhibiting stable break loads, high elongation at break, and good ductility. In contrast, very high printing speeds (e.g., 80 mm/s) reduced tensile strength to below 55.61 MPa, while very low speeds (e.g., 40 mm/s) also lowered tensile strength, likely due to excessive heat accumulation that weakened layer adhesion. Moderate printing speeds promoted a more uniform stress distribution, reducing premature failure, whereas high-speed prints showed weaker layer bonding and low-speed prints experienced thermal stress and warping.

Surface roughness analysis further revealed that decreasing printing speed led to lower Ra, Rz, and Rq values, supporting the hypothesis that slower deposition improves surface quality through enhanced material deposition and substrate cooling. However, a trade-off was observed, as excessively high print speeds degraded surface finish and only provided strength benefits up to a certain threshold.

This non-linear behavior is consistent with the mixed findings in the literature. Some studies have reported that higher printing speeds negatively affect surface quality and stability by increasing porosity and roughness while decreasing extrusion volume [36]. Conversely, other research has suggested that lower velocities promote interlayer bonding, whereas higher velocities generate thermal stresses detrimental to material strength [37]. These differing outcomes highlight the complex interplay between printing speed, thermal effects, and mechanical performance, which explains the nonconsistency observed in the present results. Therefore, based on these findings, the hypothesis that printing speed and orientation have no statistically significant effect on the mechanical properties and surface quality of 3D-printed PLA samples was rejected.

CONCLUSIONS

- Print orientation significantly influences the mechanical properties of 3D-printed parts, such as tensile strength, toughness, and Young's modulus, which are critical for structural integrity and performance.
- Samples with layers oriented parallel to the applied force (0° orientation) exhibited superior tensile strength, while those printed at a 90° orientation showed reduced strength due to weaker interlayer bonding.
- Toughness is enhanced in the 0° orientation due to its combination of strength and ductility, allowing it to absorb higher energy before failure, whereas the 90° orientation is more prone to interlayer fractures under tensile stress.
- The anisotropic nature of FDM-printed parts is evident in the variation of Young's modulus, with 90° orientation samples showing lower stiffness compared to 0° orientation samples.
- A clear correlation between print speed and surface roughness was observed, where slower print speeds produced smoother surfaces and improved the overall quality of the parts.

- A print speed range of 50–70 mm/s was identified as optimal for achieving a balance between surface finish and tensile strength in PLA parts, ensuring strong interlayer bonding and smooth surfaces.
- In high-performance applications, such as aerospace, automotive, and medical devices, optimized print orientation and speed enhance production efficiency by improving mechanical performance and reducing surface imperfections.
- The flexibility of 3D printing enables customization of parameters to achieve specific requirements, allowing the production of parts tailored to prioritize either surface finish or mechanical strength, depending on the application.

ACKNOWLEDGEMENT

The authors would like to thank De Montfort University, United Kingdom, and Satbayiev University, Kazakhstan, for their financial and institutional support in the completion of this research. Their contributions have been instrumental in facilitating this work, and we deeply appreciate their commitment to academic collaboration and innovation.

REFERENCES

1. Z. Ross, 2023. 3D Printing for Beginners: A Step-by-Step Guide to Getting Started. 3D Printing Book.
2. S. Rouf, A. Raina, M. Irfan Ul Haq, N. Naveed, S. Jeganmohan, A. Farzana Kichloo, 2022. 3D printed parts and mechanical properties: Influencing parameters, sustainability aspects, global market scenario, challenges and applications. Advanced Industrial and Engineering Polymer Research, 5(3), 143–158. https://doi.org/10.1016/j.aiepr.2022.02.001
3. K. S. Prakash, T. Nancharaih, V. V. S. Rao, 2018. Additive Manufacturing Techniques in Manufacturing - An Overview. Materials Today: Proceedings, 5(2 Pt 1), 3873–3882. https://doi.org/10.1016/j.matpr.2017.11.642
4. D. Turney, 2021. History of 3D Printing: It's Older Than You Think. Autodesk.com. https://www.autodesk.com/design-make/articles/history-of-3d-printing
5. N. Rafiq, 2017. 3D Printing: Technology, Applications, and Selection. https://www.taylorfrancis.com/books/mono/10.1201/9781315155494/3dprinting-rafiq-noorani
6. S. Muller, E. Westkamper, 2018. Modelling of Production Processes: A Theoretical Approach to Additive Manufacturing. Procedia CIRP, 72, 1524–1529.
7. K. Solberg, J. Torgersen, F. Berto, 2020. Fatigue Behaviour of Additively Manufactured Inconel 718 Produced by Selective Laser Melting. Procedia Structural Integrity, 13, 1762–1767.
8. Y. Xu, H. Zhang, B. Savija, S.C. Figueiredo, E. Schlangen, 2019. Deformation and fracture of 3D printed disordered lattice materials: Experiments and modeling. Materials and Design, 162, 143–153.
9. J. Allum, A. Gleadall, V.V. Silberschmidt, 2020. Fracture of 3D-printed polymers: Crucial role of filament-scale geometric features. Engineering Fracture Mechanics, 224, 106818.
10. G. Qian, Z. Jian, X. Pan, F. Berto, 2020. In-situ investigation on fatigue behaviors of Ti-6Al-4V manufactured by selective laser melting. International Journal of Fatigue, 133, 105424.

11. O.H. Ezeh, L. Susmel, 2020. On the notch fatigue strength of additively manufactured polylactide (PLA). International Journal of Fatigue, 136, 105583.
12. M.R. Khosravani, T. Reinicke, 2020. On the environmental impacts of 3D printing technology. Applied Materials Today, 20, 100689.
13. Y. Luo, X. Lin, X. Wan, Z. Wang, P. Huang, 2020. 3D printing of hydrogel scaffolds for future application in photothermal therapy of breast cancer and tissue repair. Acta Biomaterialia, 92, 37–47.
14. M.R. Khosravani, T. Reinicke, 2020. Effects of raster layup and printing speed on strength of 3D-printed structural components. Procedia Structural Integrity, 28, 720–725. https://doi.org/10.1016/j.prostr.2020.10.083
15. E. Bayas, P. Kumar, K. Deshmukh, 2024. Review of process parameter's effect on 3D printing. GIS-Zeitschrift für Geoinformatik, 10, 834–845.
16. V. Shiva, S.N.R. Vangala, P. Oshin, S. Babu, S. Janbhasha, C. Smitha, P. Kumar, Y. Raju, 2024. Optimization of Manufacturing Parameters of PLA Components Using Taguchi and Neural Network (NN) Technique. Advance Sustainable Science Engineering and Technology, 20, 405–412.
17. M. Issametova, N.V. Martyushev, A. Zhastalap, L.B. Sabirova, U. Assemgul, A. Tursynbayeva, G. Abilezova, 2024. Determination of Residual Stresses in 3D-Printed Polymer Parts. Polymers, 16, 2067. https://doi.org/10.3390/polym16142067
18. J. Li, S. Yang, D. Li, V. Chalivendra, 2019. Numerical and experimental studies of additively manufactured polymers for enhanced fracture properties. Engineering Fracture Mechanics, 204, 557–569.
19. C. Madhav, R. Sri, N. Kesav, Y. Narayan, n.d. Importance and Utilization of 3D Printing in Various Applications.
20. M.-H. Hsueh et al., 2021. Effect of Printing Parameters on the Tensile Properties of 3D-Printed Polylactic Acid (PLA) Based on Fused Deposition Modeling. Polymers, 13(14), 2387. https://doi.org/10.3390/polym13142387
21. K.M. Panchasara, A.N. Ramakrishnan, K. Mehle, C. Ludtka, S. Schwan, 2022. Modeling of Manufacturing Induced Residual Stress in 3D Printed Components. Symp, 403, 2100465.
22. Z. Wang, F. Zhao, F. Fuh, L. Lee, 2019. Effect of Porosity on Mechanical Properties of 3D Printed Polymers: Experiments and Micromechanical Modeling Based on X-Ray Computed Tomography Analysis. Polymers, 11(7), 1154. https://doi.org/10.3390/polym11071154
23. A.A. Ansari, M. Kamil, 2021. Effect of print speed and extrusion temperature on properties of 3D printed PLA using fused deposition modeling process. Materials Today: Proceedings, 45, 137. https://doi.org/10.1016/j.matpr.2021.02.137
24. H. Alzyod, P. Ficzere, 2023. Correlation Between Printing Parameters and Residual Stress in Additive Manufacturing: A Numerical Simulation Approach. Production Engineering Archive, 29, 279–287.
25. A.V. Balashov, M.I. Markova, 2019. Study of the structure and properties of products produced by 3D printing. Engineering Bulletin of Don, 1, 5618.
26. C. Casavola, A. Cazzato, V. Moramarco, C. Pappalettere, 2016. Orthotropic mechanical properties of fused deposition modelling parts described by classical laminate theory. Materials & Design, 90, 453–458. https://doi.org/10.1016/j.matdes.2015.11.009
27. O.A. Mohamed, S.H. Masood, J.L. Bhowmik, 2015. Optimization of fused deposition modelling process parameters: a review of current research and prospects. Advances in Manufacturing, 3(1), 42–53. https://doi.org/10.1007/s40436-014-0097-7

28. B.M. Tymrak, M. Kreiger, J.M. Pearce, 2014. Mechanical properties of components fabricated with open-source 3-D printers under realistic environmental conditions. Materials & Design, 58, 242–246. https://doi.org/10.1016/j.matdes.2014.02.038

29. K.V. Wong, A. Hernandez, 2012. A Review of Additive Manufacturing. ISRN Mechanical Engineering, 2012, 1–10. https://doi.org/10.5402/2012/208760

30. H. Tekinalp, V. Kunc, G.M. Vélez-García, C. Duty, L.J. Love, A.K. Naskar, C.A. Blue, S. Ozcan, 2014. Highly oriented carbon fiber–polymer composites via additive manufacturing. Composites Science and Technology, 105, 144–150. https://doi.org/10.1016/j.compscitech.2014.10.009

31. D. Hidalgo-Carvajal, A. Muñoz, J.J. Garrido-González, R. Carrasco-Gallego, V. Alcázar, 2023. Recycled PLA for 3D Printing: A Comparison of Recycled PLA Filaments from Waste of Different Origins after Repeated Cycles of Extrusion. Polymers, 15(17), 3651. https://doi.org/10.3390/polym15173651

32. N. Ayrilmis, M. Kariz, J.H. Kwon, M. Kitek Kuzman, 2019. Effect of printing layer thickness on water absorption and mechanical properties of 3D-printed wood/PLA composite materials. The International Journal of Advanced Manufacturing Technology, 102(5–8), 2195–2200. https://doi.org/10.1007/s00170-019-03299-9

33. T. Koslow, 2018. 2019 PLA Filament Guide – All You Need to Know. All3DP, Apr. 17. https://all3dp.com/1/pla-filament-3d-printing/

34. A. Locker, 2017. 12 Vital Facts About Food Safe 3D Printing. All3DP, May 20. https://all3dp.com/1/food-safe-3d-printing-abs-pla-food-safe-filament/

35. S. Wang, Y. Ma, Z. Deng, S. Zhang, J. Cai, 2020. Effects of fused deposition modeling process parameters on tensile, dynamic mechanical properties of 3D printed polylactic acid materials. Polymer Testing, 86, 106483. https://doi.org/10.1016/j.polymertesting.2020.106483

36. S. Saefudin, S. Raharjo, S. Syarifudin, P. Purnomo, M. Rusydi, A. Kuzmin, M. Subri, M. Pujianto, 2025. A Review of Factors Affecting the Mechanical Performance of PLA in FDM 3D Printing. Advance Sustainable Science Engineering and Technology, 7, 0250208. https://doi.org/10.26877/chs1gc62

37. J.A. Afonso, J.L. Alves, G. Caldas, B.P. Gouveia, L. Santana, J. Belinha, 2021. Influence of 3D printing process parameters on the mechanical properties and mass of PLA parts and predictive models. Rapid Prototyping Journal, 27(3), 487–495.